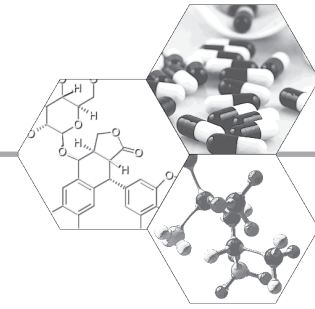

Molecular dynamics simulations and docking studies on 3D models of the heterodimeric and homodimeric 5-HT_{2A} receptor subtype

Background: G-protein coupled receptors may exist as functional homodimers, heterodimers and even as higher aggregates. In this work, we investigate the 5-HT_{2A} receptor, which is a known target for antipsychotic drugs. Recently, 5-HT_{2A} has been shown to form functional homodimers and heterodimers with the mGluR2 receptor. The objective of this study is to build up 3D models of the 5-HT_{2A}/mGluR2 heterodimer and of the 5-HT_{2A}-5-HT_{2A} homodimer, and to evaluate the impact of the dimerization interface on the shape of the 5-HT_{2A} binding pocket by using molecular dynamics simulations and docking studies. **Results and discussion:** The heterodimer, homodimer and monomeric 5-HT_{2A} receptors were simulated by molecular dynamics for 40 ns each. The trajectories were clustered and representative structures of six clusters for each system were generated. Inspection of the these representative structures clearly indicate an effect of the dimerization interface on the topology of the binding pocket. Docking studies allowed to generate receiver operating characteristic curves for a set of 5-HT_{2A} ligands, indicating that different complexes prefer different classes of 5-HT_{2A} ligands. **Conclusion:** This study clearly indicates that the presence of a dimerization interface must explicitly be considered when studying G-protein coupled receptors known to exist as dimers. Molecular dynamics simulation and cluster analysis are appropriate tools to study the phenomenon.

It is now well established that many G-protein coupled receptors (GPCRs) homo- or heterodimerize under physiological conditions [1–5]. The notion that GPCRs may exist as homo- or heterodimers allows for a re-interpretation and better comprehension of some of the pharmacological inconsistencies that have, so far, characterized the research in the GPCR field [6]. A particularly interesting case is given by the serotonin 5-HT_{2A} receptor subtype. The 5-HT_{2A} receptor subtype is well-characterized pharmacologically and its activation by agonists produces a phenotype that is consistent with many features predicted by the serotoninergic hypothesis of schizophrenia. However, there are also inconsistencies that apparently challenge this hypothesis. Notable is the observation that distinct sets of 5-HT_{2A} agonists, classified as hallucinogen (HC) or nonhallucinogen (NHC) compounds, act at the same site of the receptor while displaying substantially different phenotypic effects on behavior [7–9]. In the attempt to reconcile this observation with the serotoninergic hypothesis, in 2007, Gonzalez-Maeso and coworkers proposed that HCs and NHCs, albeit acting at the same serotoninergic site, can activate different intracellular pathways by selecting different receptor conformational states in agreement with the theory of the agonist trafficking of receptor signaling [9,10]. In 2008, Gonzalez-Maeso *et al.* reported that, in some neurons, 5-HT_{2A} and the metabotropic glutamate receptor subtype mGluR2 physically interact to form a functional heterodimer, with relevant consequences on the mechanism of action of antipsychotic drugs [11,12]. In the absence of mGluR2 agonists, the heterocomplex induces psychotic behavior, while in the presence of the mGluR2 agonists the heterocomplex reduces or blocks the hallucinogenic behavior [11,12]. More recently, it has been shown that the 5-HT_{2A} receptor can also constitutively aggregate to form homodimers or homo-oligomers and a three-state receptor dimer model has been proposed [13]. This model explains the asymmetrical behavior of each 5-HT_{2A} protomer through the existence of one inactive and two active states of the complex and Rovira *et al.* hypothesized that each active state is able to select and interact with different intracellular effectors [14].

The identification of functional heterodimers and homodimers thus offers a unique possibility to revise the pharmacology of HCs and NHCs in the context of their ability to select individual, yet uncharacterized, dimeric states

Agostino Bruno[‡], Claudia Beato[‡] & Gabriele Costantino[†‡]

[‡]Dipartimento Farmaceutico, Via G. P. Usberti 27/A, Campus Universitario, Università degli Studi di Parma, 43100 Parma, Italy
[†]Author for correspondence:
Tel.: +39 052 190 5054
E-mail: gabriele.costantino@unipr.it

FUTURE SCIENCE part of fsg

Key Terms

Dimerization interface: Physical surface of contacts between the two protomers forming a homodimer or heterodimer.

Cluster analysis: Assignment of a series of observations into classes, which contain similar observations, according to a given parameter.

that in turn can activate (or repress) individual intracellular effector pathways. Until now, the 5-HT_{2A} receptor was considered and studied as monomeric entity mainly through homology modeling studies [15,16], while the identification of the complexity of the 5-HT_{2A} architecture also offers new challenges for medicinal and computational chemists to build up reliable and predictive models of homo- or hetero-complexes. In previous work, we started to address some of these issues by generating a 3D model of the 5-HT_{2A}–mGluR2 complex and by analyzing it through molecular dynamics (MD) simulations [17]. In particular, we were able to clearly identify the effect of the heterodimerization interface on the shape of the binding pocket of the 5-HT_{2A} protomer. The results provided a molecular ground for discussing the reported allosteric effect of mGluR2 on 5-HT_{2A}-mediated response and suggested that heterocomplex can be a more suitable target for *in silico* screening than the monomeric protomer.

As a continuation of our work in this field, we now report the direct comparison between the two dimeric forms of the 5-HT_{2A} receptor assigned with functional relevance, namely the heterodimeric mGluR2–5-HT_{2A} and the homodimeric 5-HT_{2A}–5-HT_{2A}. The two dimeric complexes, both in their apo form, were simulated by MD for 40 ns each. The results were analyzed and compared in order to check the effect of different **dimerization interfaces** on the shape and size of the putative serotoninergic binding pocket. Finally, we also report docking studies on selected representative structures for each 5-HT_{2A} receptor forms and we assess the ability of each conformational state to recognize different classes of 5-HT_{2A} ligands.

Table 1. Parameters used for embedding the homodimer complex into the phospholipidic bilayer.

Box type	Rectangle		
System size	x	y	z
	88.525	115.25	112.181
Crystal angle	α	β	γ
	90.0	90.0	90.0
Number of lipids	260		
System building options	Replacement method		
Component building options	Water box	Include ions (0.15-M KCl)	
Number of atoms	114,960		
Number of waters	24,526		
Lipids	Dimyristoylphosphatidylcholine		

Experimental section

■ Construction of the molecular systems & MD simulations

The mGluR2–5-HT_{2A} heterodimer was built, as described previously [17]. The 5-HT_{2A}–5-HT_{2A} homodimer was built by using a 5-HT_{2A} protomer constructed by homology modeling, as previously described [17]. In the next sections, we refer to the protomers of the homodimer complex as protomerA (ProA) and protomerB (ProB). The homodimerization interface was modeled as a TM4/TM5 interface, and constructed by selecting a Rosetta++ output structure after visual inspection of geometrical parameters. The homodimer, the heterodimer and a protomeric monomer were then subjected to MD simulation, using the experimental conditions previously described [17] and summarized in **Tables 1 & 2**.

■ MD analysis & cluster analysis

All the MD trajectories were analyzed with visual molecular dynamics [18]. Ideally, a long MD simulation allows sampling of the whole conformational space for the molecular system under investigation. Root-mean-square deviation (RMSD) clustering of individual snapshots along the MD simulation allows one to evaluate the degree of sampling and, thus, the goodness of the MD simulation [19]. The representative structures of each cluster can ideally be considered models of individual conformational states for a given system. In addition, these structures can be used for docking studies [20–23], thus expecting to give hints on the ligand's ability to select individual conformational states. We are aware that 40-ns MD simulations certainly cannot be considered sufficient to cover the whole conformational state of a dimeric receptor embedded in a phospholipidic bilayer. We therefore concentrated our attention on changes that take place around the putative binding pocket of 5-HT_{2A}, and the **cluster analysis** was therefore carried out by comparing a series of residues lining up the binding pocket. In detail, we performed the cluster analysis by using the *ptraj* tool of Amber9 [101] and the average-linkage algorithm [19]. The representative structure of each cluster, dumped by *ptraj* in the output file, represents the structure closest to the average structure, and it can be considered a sort of centroid of the cluster, which retains the average properties of the cluster [19,101]. For each 40-ns simulation, 2000 snapshots were collected and clustered according to RMSD of the

Table 2. Parameters used for the molecular dynamics equilibration and production phases.

	Timestep (fs)	Numstep (fs)	Temperature (K)	Harmonic constraints (Kcal/mol)					Constant temperature control
				Backbone	Sidechains	Lipids	Waters	Ions	
Equilibrations steps									
Step 1	1.0	2500	300	50	50	50	50	50	NVT
Step 2	1.0	2500	300	10	10	10	5	5	NVT
Step 3	1.0	5000	310	10	10	10	5	5	NVT
Step 4	1.0	5000	310	10	5	10	5	5	NVT
Step 5	1.0	25000	310	2.5	2.5	2.5	1.0	1.0	NVT
Step 6	1.0	25000	310	2.5	1	2.5	1	2.5	NVT
Step 7	1.0	25000	310	-	-	-	-	-	NVT
Simulation									
Step 7	1.0	40 ns	310	-	-	-	-	-	NPT p = 1.01325 bar

backbone, and CB and CG atoms of the residues lining up the serotoninergic binding pocket ($D^{3.32}$, $S^{3.36}$, $T^{3.37}$, $S^{5.43}$, $S^{5.46}$, $W^{6.48}$, $F^{6.51}$, $F^{6.52}$ and $Y^{7.43}$ [17,24–31]; superscripts indicate Ballestreros–Weinstein numbering for conserved GPCR residues [32]).

In order to assess the performance of a cluster analysis, several indices or clustering metrics can be used, such as the Davies–Bouldin index, the pseudo F-static, the ratio sum of squares regression/total sum of squares explaining the percentage of variance of the data and the critical distance [19,101]. In particular, in the paper by Shao *et al.*, it is proposed that the use of different metrics when analysing the results of a cluster analysis is an appropriate way to assess the quality of the cluster [19]. In our work, we used the ratio sum of squares regression/total sum of squares and the critical distance as metrics in order to evaluate the quality of our tree of cluster. Furthermore, the obtained clusters were then analyzed by visual inspection (the values for the metrics used to assess the performance of our cluster analysis are reported in [SUPPLEMENTARY TABLE 1]). We performed several cluster analyses and, on the basis of the collected data, we selected the best parameters to cluster our simulations. For each MD simulation (5-HT_{2A}–mGluR2 heterodimer complex, 5-HT_{2A} and 5-HT_{2A}–5-HT_{2A} homodimer complex), we choose to cut our tree of clusters at six representative clusters.

■ Docking studies

A set of known 5-HT_{2A} ligands was selected from the GPCR-Ligand Database [33,102] and from data reported in the literature [24–31,34–40]. The set of active 5-HT_{2A} ligands consists of nine HCs; nine NHCs and nine antagonists [SUPPLEMENTARY TABLE 2]. The set of 27 active 5-HT_{2A} ligands was enriched by 73 additional chemotypes obtained from a Schrödinger Library and from the International Union of Basic and Clinical Pharmacology database [41,103,104, SUPPLEMENTARY TABLE 3]. The idea is to enrich the active set with chemotypes displaying common structural features with the selected 5-HT_{2A} ligands (similar molecular weight, number of nitrogens, number of oxygens and number of rings) but not reported to be active at the 5-HT_{2A} receptor subtype. The main aim of this part of the work was to verify whether considering several conformational states of the receptor would have an impact on the results of the docking studies. With regards to this aim, we selected, for each system, the representative structure of the first cluster as representative of the initial state of the system and the representative structure of the most populated cluster as representative of the most favored state for that simulation. Thus, eight different conformational states of the 5-HT_{2A} receptor were selected (two for the monomer, two for the 5-HT_{2A} complexed with the mGluR2 receptor, two for the ProA and two for the ProB) and employed in the docking studies with 100 ligands (23 known active compounds and 73 classified as inactive compounds). As a first attempt, we carried out rigid docking runs, but the results were inconclusive (data not shown), possibly because the representative structures were selected out of MD simulations carried out on apo states. Thus, we decided to introduce flexibility by developing a protocol based on the induced-fit docking (IFD) tool available in Maestro [41,103].

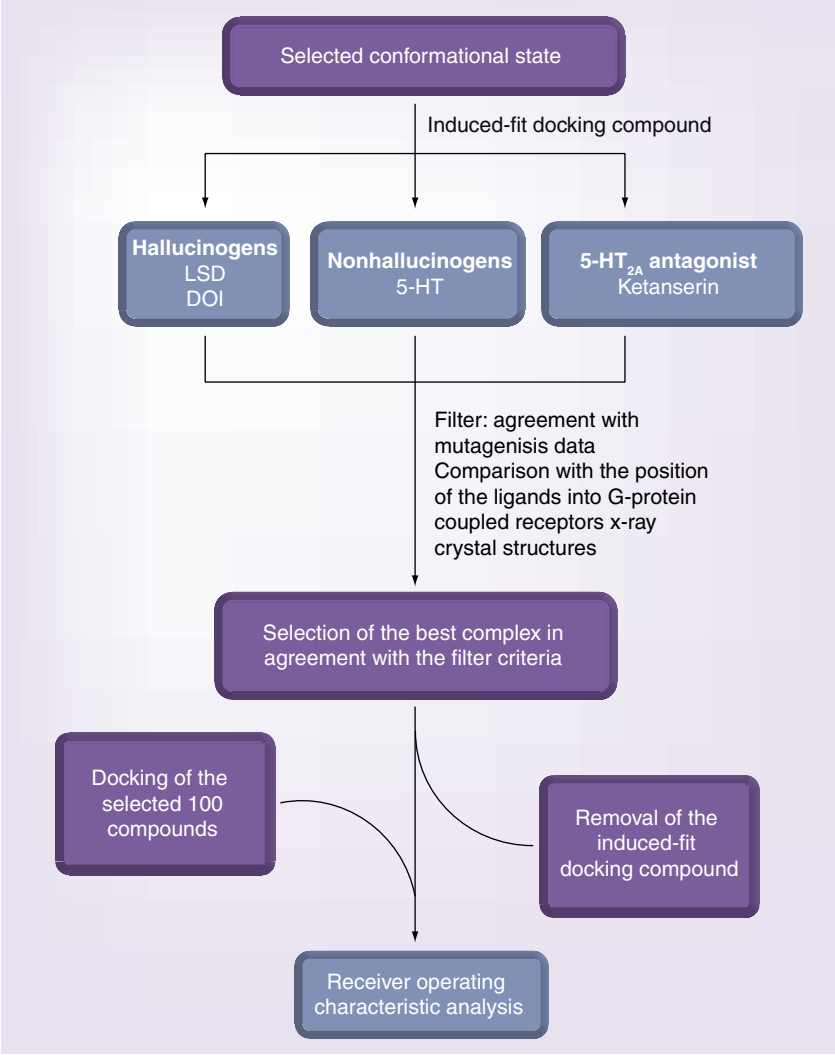

Figure 1. Protocol used for the docking studies.

Briefly, the protocol, summarized in **Figure 1**, is based on the IFD of selected ligands into representative structures of the receptor. The resulting complexes will have a modified binding pocket with respect to the apo simulation that will be more prone to accommodate all the remaining ligands through rigid docking.

Table 3. Selected complexes from the induced-fit docking analysis.

Structures	Ligands
Representative structure cluster 1 monomer	Serotonin
Representative structure most populated cluster monomer	Ketanserin
Representative structure cluster 1 5-HT_{2A}–mGluR2	Serotonin
Representative structure most populated cluster 5-HT_{2A}–mGluR2	LSD
Representative structure cluster 1 5-HT_{2A}–ProA	Ketanserin
Representative structure most populated cluster 5-HT_{2A}–ProA	Ketanserin
Representative structure cluster 1 5-HT_{2A}–ProB	Serotonin
Representative structure most populated cluster 5-HT_{2A}–ProB	DOI

This chosen protocol is intended to be a compromise between explicit treatment of flexibility and manageable computational time. Clearly, the use of the IFD protocol adds complexity to the study as the choice of a given ligand for a particular conformational state of the receptor in the IFD may well bias the subsequent rigid docking. Furthermore, there can be the possibility that the minimization procedure of the IFD will hide the differences resulting from the MD evolution. Also, by taking into account these possible drawbacks, the protocol described in **Figure 1** is based on the choice of a representative chemotype of each class of the 5-HT_{2A} ligand for initial IFD. The IFD results were evaluated, for each conformational states, on the basis of the adherence of the obtained poses to available mutagenesis data [17,24–31] and to the pose experimentally determined for other GPCR receptors [42–45]. Thus, we carried out a total of 32 IFD runs (four ligands for two different conformational states, initial and most populated ones, for four different receptor states, monomer, heterodimer, ProA and ProB). The 32 IFD complexes were evaluated for their agreement with experimental data and eight complexes were selected **(Table 3)**. These complexes were used for the subsequent rigid docking runs. The obtained poses were ranked according to their G-score and the corresponding receiver operating characteristic (ROC) curves [46] generated for each class of ligands, for the representative structures of the most populated clusters.

In detail, the initial docking site was defined by a box of 18 × 18 × 18 Å centered on $D^{3.32}$; $S^{3.36}$, $T^{3.37}$, $S^{5.43}$, $S^{5.46}$, $W^{6.48}$, $F^{6.51}$, $F^{6.52}$ and $Y^{7.43}$, and no interaction constraints were used, according to the protocol depicted in **Figure 1**. The van der Waals' scaling factor was set to 0.8. Only the docking poses in agreement with filter criteria were retained. As filter criteria, we used the agreement with mutagenesis data and comparison of the obtained poses with the position of the ligand into available GPCRs x-ray crystal structures **(Figure 1)**.

In the second stage of the study, the whole set of 100 compounds (27 active and 73 inactive ones) was docked into the eight structures selected by the IFD protocol, keeping the same Glide grid of the selected IFD ligand–receptor complex. The ligands were ranked by their Glide Score and one pose per ligand was collected and a ROC analysis [46] were performed using four different schemes of ligand classification:

- 5-HT$_{2A}$ active ligands (27 compounds) versus the decoy set (73 compounds);
- 5-HT$_{2A}$ agonists (18 compounds) versus decoy set enriched by the nine 5-HT$_{2A}$ antagonists (82 compounds);
- 5-HT$_{2A}$ antagonists (nine compounds) versus decoy set enriched by the 18 5-HT$_{2A}$ agonists (91 compounds);
- HCs (nine compounds) versus decoy set enriched by the 5-HT$_{2A}$ NHCs and antagonists (91 compounds). In order to understand if particular conformational states preferentially interact with one class of 5-HT$_{2A}$ ligands, the area under the curve and the enrichment factors at 2, 5, 10 and 20% were computed for each ROC plot.

Results & discussion

■ MD & cluster analysis

FIGURE 2A shows the trajectories of the four systems under study, color-coded according to the six chosen clusters. **FIGURE 2B** shows the relative percentage of population of each cluster. It can be appreciated as the clusters are differently populated and in some cases the trajectory explores conformational states belonging to the same cluster during the simulation.

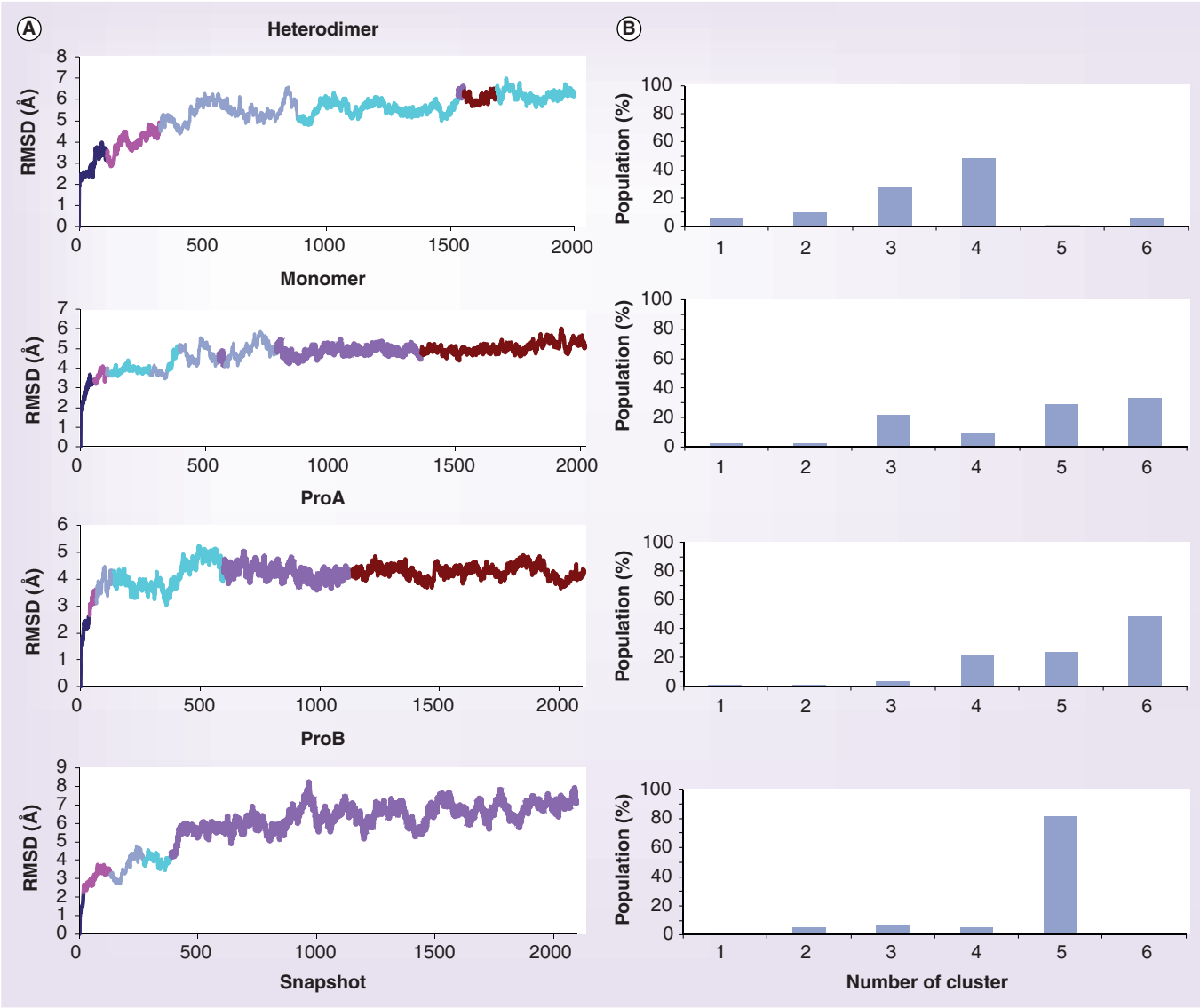

Figure 2. 2000 snapshots covering 40 ns per simulation have been collected and clustered according to root-mean-square deviation from the starting structure. (A) Snapshots belonging to individual clusters have been color coded and projected on the root-mean-square deviation plot of the trajectories. Dark blue: cluster 1; pink: cluster 2; light purple: cluster 3; light blue: cluster 4; dark purple: cluster 5; brown: cluster 6. **(B)** Percentage of population of each cluster for each simulation.

Table 4. Average root-mean square-deviation (Å) fluctuations for the Cα atoms of selected residues lining up the binding pocket of the 5-HT_{2A}.

	5-HT_{2A} monomer	5-HT_{2A} into heterodimer	ProtomerA	ProtomerB
D3.32	1.41	1.58	2.05	2.09
S3.36	0.85	1.49	1.94	1.95
T3.37	0.68	1.45	1.86	1.79
S5.43	3.31	1.58	1.45	2.09
S5.46	1.72	1.06	1.38	1.80
W6.48	2.75	1.96	1.41	2.02
Y7.43	1.93	1.11	1.97	2.52
F6.51	3.10	2.46	1.56	2.21
F6.52	5.21	3.47	1.73	2.69

This is the case for 5-HT_{2A} extracted from the heterodimer simulation, or 5-HT_{2A} simulated as a monomer. Noteworthy is the case of the homodimer simulation, in which the two protomers show very different behaviors. This is an interesting observation since the homodimer represents a theoretical isotropic system, where each protomer is embedded in the same environment. Quite unexpectedly, when the trajectory extracted for ProB is clustered, we obtained only one large cluster that covers approximately 80% of the whole simulation. Conversely, in the case of ProA the population of the clusters is more evenly distributed around the last three ones **(Figure 2A & B)**. The different results of the cluster analysis for the ProA and ProB is indicative that the homodimer does not evolve, under our simulation conditions, in a symmetric way. The nonsymmetric evolution of the homodimer simulation suggests that the interactions at the homodimer interface are thus anisotropic and this is in agreement with the experimental evidence that one protomer is able to allosterically affect the behavior of each other protomer into the complex [11–13].

■ Analysis of the binding pocket

We have previously shown that the heterodimerization interface impacts the shape of the binding pockets of 5-HT_{2A} when simulated in the heterocomplex with mGluR2 [17]. We now extend these previous results to a 40-ns simulation of the homodimer 5-HT_{2A}–5-HT_{2A} complex. Thus, we analyzed nine residues known to be involved in 5-HT_{2A} ligand recognition, namely $D^{3.32}$, $S^{3.36}$, $T^{3.37}$, $S^{5.43}$, $S^{5.46}$, $W^{6.48}$, $F^{6.51}$, $F^{6.52}$ and $Y^{7.43}$ [17,24–31]. **Table 4** reports the average RMSD per residue of the above mentioned residues for the 5-HT_{2A} protomer unit extract from the heterocomplex with mGluR2, for the monomeric form of the 5-HT_{2A} receptor and for the two 5-HT_{2A} protomers extracted from the homodimer.

The analysis of the average RMSD values per residue **(Table 4)** clearly indicates the dependency of the binding pocket shape upon the simulation conditions. In particular, the key residues S5.43, S5.46, experimentally known to be involved in HCs binding [30], and the residues F6.51 and F6.52 display significantly different displacement when 5-HT_{2A} is simulated as a monomer, or part of a homodimer or heterodimer. Also the overall shape of the binding pocket changed during the simulation. Thus, **Figure 3A–H** shows the shape of the binding pocket and the surface-accessible pocket around the binding site of the representative structures of the initial and most populated clusters for each of the four system. This analysis was made using the CASTp server [105]. In **Table 5** we report the values of the area (Å^2) and volume (Å^3) for each structure reported in **Figure 3**. The data reported in **Table 5** highlight that the area and volume of the accessible pockets and of the binding pocket constantly increase in a time simulation-dependent manner.

A particular comment deserves the high fluctuation **(Table 4)** displayed by the $W^{6.48}$, $F^{6.51}$ and $F^{6.52}$ residues. These residues are located in a region of TM6 characterized by high flexibility [47] and, in particular, they are located one turn above the MWCP microdomain, which corresponds to the known CWxP domain, conserved among several GPCRs of class A, **(Figure 4A)** and characterized by high flexibility.

In fact, the superimposition of TM6 of the representative structures of the six clusters of each simulation **(Figure 4B)** indicates a wide oscillation of the terminal cap of TM6 induced by different movement of the microdomain. The oscillation is much larger in the case of the 5-HT_{2A} simulation as a monomer than in the case of the mGluR2–5-HT_{2A} and 5-HT_{2A}–5-HT_{2A} simulations. Therefore, it is clear that the presence and the type of dimerization interface visibly impact the flexibility of the TM6 helix.

This is particularly relevant, since $F^{6.51}$, $F^{6.52}$ and $W^{6.48}$ form a hydrophobic pocket conserved among class A of the GPCRs [47], especially for the subfamily of the biogenic amines. It has been hypothesized that these residues may play a crucial role in the activation mechanism for a GPCR, by triggering the conformational change required for receptor activation [48] and ligand recognition [8].

While the recent resolution of the hypothetical active states of opsin, turkey β1- and human β2-adrenergic receptors (PDB code: 3DQB, 3CAP, 3P0G, 3PDS and 2Y00-2Y04, respectively) indicates only a minor difference in the orientation of W6.48 with respect to the resting state of the same receptor **(Table 6)**, other aromatic residues (conserved positions 5.44, 5.47 and 5.48) undergo more significant displacement in their chi1 and chi2 torsional angles between active and resting state structures **(Table 6)**.

The chi1 and chi2 values for the residues in the same conserved positions for the six representative structures extracted from each system are shown in [Supplementary Table 4]. Since the representative structures of the most populated cluster can be seen as models of the conformational states along which the systems evolve under the simulation condition, we can state that depending on the presence and on the type of the dimerization interface, our molecular systems differently populate conformational states potentially relevant for ligand binding and receptor activation. Clearly, these data must be interpreted in the light of the short simulation time (40 ns), which does not allow the sampling of the whole conformational state. What should be stressed here is that the residues forming the hydrophobic pockets showed a dynamical behavior and the sidechains flipped in a short timescale. These

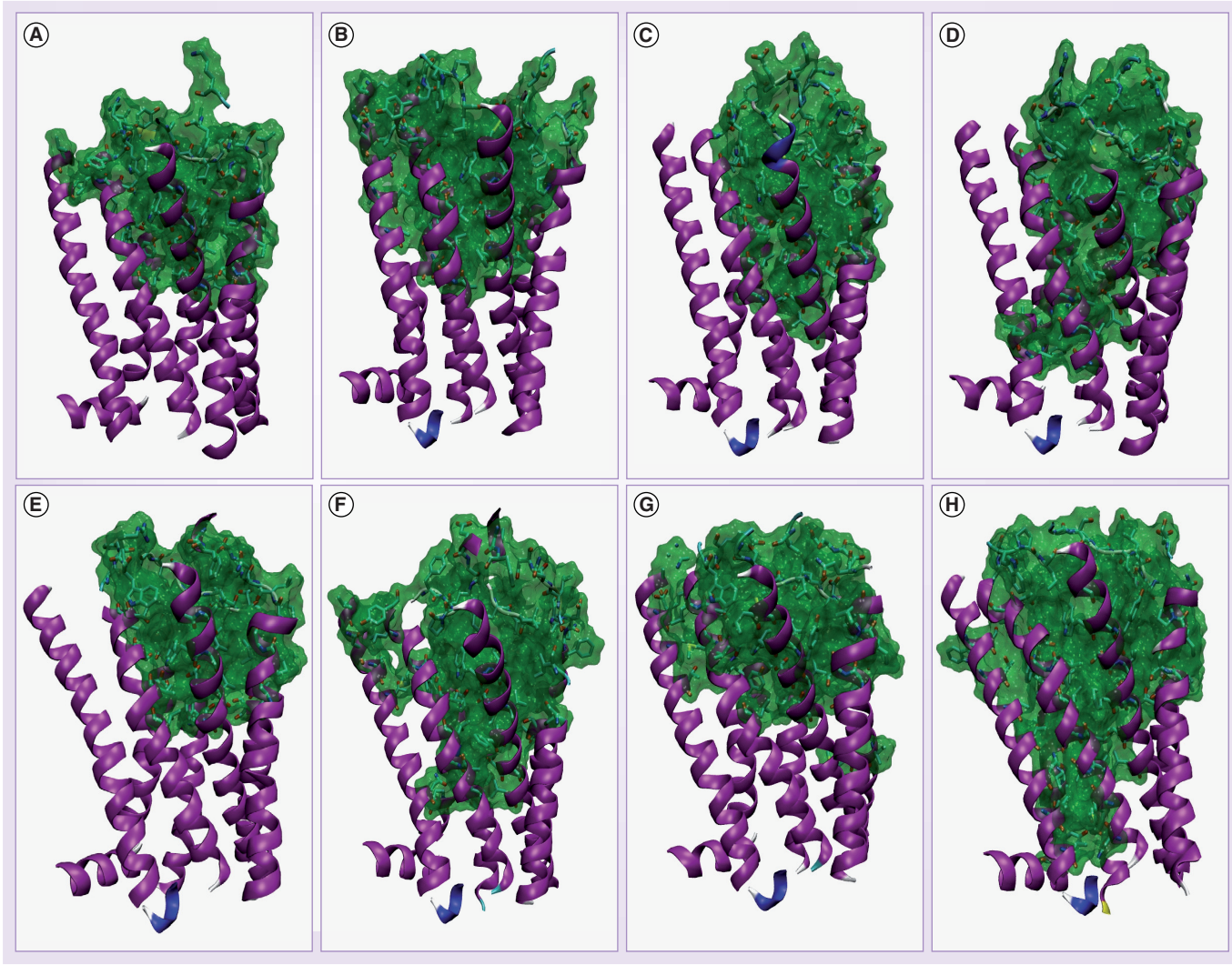

Figure 3. Surface-accessible pockets and cavities. (A) Representative structure of the cluster 1 for the 5-HT_{2A} simulation as monomer. **(B)** Representative structure of the most populated cluster for the 5-HT_{2A} simulation as monomer. **(C)** Representative structure of the cluster 1 for the 5-HT_{2A}–$mGlu_{R2}$ simulation. **(D)** Representative structure of the most populated cluster for the 5-HT_{2A}–mGluR2 simulation. **(E)** Representative structure of the cluster 1 for the 5-HT_{2A}–protomerA (ProA). **(F)** Representative structure of the most populated cluster for the 5-HT_{2A}–ProA. **(G)** Representative structure of the cluster 1 for the 5-HT_{2A}–protomerB (ProB). **(H)** Representative structure of the most populated cluster for the 5-HT2A–ProB.

Table 5. Values of area (Å²) and volume (Å³) of each structure reported in FIGURE 3.

Structure	Area (Å²)	Volume (Å³)	Figure
Representative structure cluster 1 monomer	2056.2	3722.1	3A
Representative structure most populated cluster monomer	2442.1	5010.4	3B
Representative structure cluster 1 5-HT$_{2A}$–mGluR2	1765.0	2666.8	3C
Representative structure most populated cluster 5-HT$_{2A}$–mGluR2	2394.5	3857.0	3D
Representative structure cluster 1 5-HT$_{2A}$–ProA	1757.2	2281.2	3E
Representative structure most populated cluster 5-HT$_{2A}$–ProA	1853	2720.4	3F
Representative structure cluster 1 5-HT$_{2A}$–ProB	1862.6	2809.2	3G
Representative structure most populated cluster 5-HT$_{2A}$–Pro	2619.5	5169.4	3H

phenomena lead to a different shape of the serotoninergic binding pocket, and the time spent of each system in an individual conformational state depends on the presence and on the type of the dimerization interface.

■ Docking of compounds

Docking studies were carried out as described in the Experimental Section. In **TABLE 3** we report the selected complexes from the IFD docking analysis. In **FIGURE 5A–C** we show, as an example, three obtained IFD complexes compared with the position of the co-crystallized ligands into available GPCR x-ray crystal structures. In **FIGURE 6A & B** we report the interaction maps for serotonin, LSD and the 5-HT$_{2A}$ binding pocket.

The results of the rigid docking runs carried out on the complexes selected by the IFD protocols **(TABLE 3)** were analyzed by generating ROC curves. Inspection of the curves **(FIGURE 7A–D,** [SUPPLEMENTARY TABLE 5]**)** revealed that in all cases the representative structure of the first clusters is not able to recognize a specific class of 5-HT$_{2A}$ ligands. An exception is given by the representative structure of the first cluster of the monomeric and of the ProA forms that were able to poorly recognize 5-HT$_{2A}$ antagonists **(FIGURE 7A & 7C)**. The comparison of the ROC curves constructed for the first representative structures and for the representative structures of the most populated clusters allowed us to clearly appreciate how each form evolve in a time-dependent manner **(FIGURES 2A–D & 7A–D)**. In fact, the monomeric and ProA forms start from a structure able to recognize 5-HT$_{2A}$ antagonists (representative structure of the first cluster, **[FIGURES 7A & C]**) and along the simulations their ability to recognize the 5-HT$_{2A}$ antagonists improved (representative structure of the most populated cluster **FIGURE 7A & C**). The heterodimeric form starts from a structure not able to recognize any 5-HT$_{2A}$ ligands (representative structure of the first cluster, **FIGURE 7B**), and evolves toward a structure able to better recognize the 5-HT$_{2A}$ agonists (representative structure of the most populated cluster, **FIGURE 7B**). ProB starts from a structure not able to recognize any 5-HT$_{2A}$ and it evolves toward a structure able to recognize different classes of 5-HT$_{2A}$ ligands **(FIGURE 7D)**, with some preference for the 5-HT$_{2A}$ antagonists.

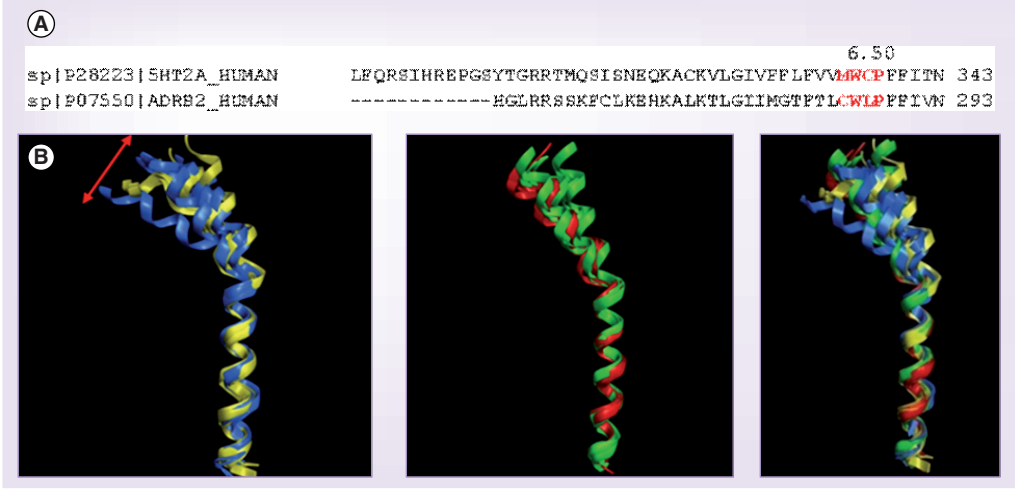

Figure 4. (A) Alignment among the TM6 human β2-adrenergic receptor and the TM6 human 5-HT$_{2A}$ receptor, highlighted in red the sequence MCWP and CWLP responsible for the bending of the TM6. **(B)** Superposition of the TM6 of the representative structure of the 5-HT$_{2A}$ protomer extracted from the heterocomplex with mGluR2 (yellow), the representative structure of 5-HT$_{2A}$ as monomer (blue), the representative structure of protomerA (green) and the representative structure of protomerB (red). The red arrow highlights the oscillatory motion of the TM6.

Table 6. Chi1 and Chi2 values for the residues forming hydrophobic clusters in the available x-ray crystal structures of G-protein coupled receptors.

	Chi1							Chi2						
Human β2-adrenergic receptor														
	S 5.43	**I 5.44**	**F 5.47**	**Y 5.48**	**W 6.48**	**F 6.51**	**F 6.52**	**S 5.43**	**I 5.44**	**F 5.47**	**Y 5.48**	**W 6.48**	**F 6.51**	**F 6.52**
2RH1	52	-73	179	-70	-73	176	-77	-	173	73	-69	106	83	96
3P0G	-66	-63	177	-56	-77	-178	-81	-	163	75	100	115	76	96
Turkey α1-adrenergic receptor														
	S 5.43	**I 5.44**	**F 5.47**	**Y 5.48**	**W 6.48**	**F 6.51**	**F 6.52**	**S 5.43**	**I 5.44**	**F 5.47**	**Y 5.48**	**W 6.48**	**F 6.51**	**F 6.52**
2VT4	18	-69	-177	-75	-86	174	-72	-	164	77	103	113	88	102
Bovine rhodopsin receptor														
	F 5.43	**V 5.44**	**F 5.47**	**I 5.48**	**W 6.48**	**Y 6.51**	**A 6.52**	**F 5.43**	**V 5.44**	**F 5.47**	**I 5.48**	**W 6.48**	**Y 6.51**	**A 6.52**
1GZM	-88	-63	-175	-60	-67	-177	-	115	-	55	-58	95	73	-
3DQB	-173	-76	177	-52	-62	-97	-	83	-	75	-71	111	121	-
3CAP	-172	-68	174	-65	-74	-121	-	79	-	70	-60	98	118	-
Human adenosine receptor A_{2A}														
	F 5.43	**F 5.44**	**V 5.47**	**L 5.48**	**W 6.48**	**L 6.51**	**H 6.52**	**F 5.43**	**F 5.44**	**V 5.47**	**L 5.48**	**W 6.48**	**L 6.51**	**H 6.52**
3EML	-178	-70	177	-174	-78	-166	-72	-139	-32	-	169	100	165	-65
Human chemokine receptor CXCR4 (3OE8)														
	I 5.43	**M 5.44**	**L 5.47**	**I 5.48**	**W 6.48**	**Y 6.51**	**Y 6.52**	**I 5.43**	**M 5.44**	**L 5.47**	**I 5.48**	**W 6.48**	**Y 6.51**	**Y 6.52**
Chain A	-52	-151	164	-59	-74	173	-71	-79	68	81	173	108	76	-56
Chain B	-57	-147	-170	-59	-72	167	-86	-56	101	65	162	100	75	-64
Chain C	-84	-154	175	-65	-78	175	-65	-67	-151	65	167	107	81	-32
Human dopamine receptor D_3														
	S 5.43	**V 5.44**	**F 5.47**	**Y 5.48**	**W 6.48**	**F 6.51**	**F 6.52**	**S 5.43**	**V 5.44**	**F 5.47**	**Y 5.48**	**W 6.48**	**F 6.51**	**F 6.52**
3PBL	64	165	-154	-61	-77	176	-82	-	-	68	-62	106	83	-96

For the serine residues the chi angle is identified by the atom types N-CA-CB-OG.
For the methionine residues, the chi angle is identified by the atom type N-CA-CB-CG1 and the chi2 angle by CA-CB-CG-SG (chi2).
For the isoleucine residues, the chi angle is identified the chi angle is identified by N-CA-CB-CG1 and the chi2 by CA-CB-CG1-CD.
For the valine residues, the chi angle is identified by N-CA-CB-CG1.
For the leucine residues, the chi angle is identified by N-CA-CB-CG and chi2 by CA-CB-CG-CD1.
For the aromatic residues, chi1 is identified by N-CA-CB-CG and chi2 by CA-CB-CG-CD1/ND1.
Highlighted in green are the residues showing the highest difference in chi1 and chi2 values.

The most interesting result is that the representative structures of the most populated cluster for each system were those best able to discriminate among the different classes of 5-HT_{2A} ligands **(Figure 7)**, with the representative structure of the most populated cluster of ProB able to recognize different kind of 5-HT_{2A} ligands. Our results clearly indicate that the different molecular systems (heterodimer, homodimer and monomer) evolve differentially during the MD simulations. This can be appreciated from ROC curves in **Figure 7**, where the initial structures of the molecular systems are compared with the respective most populated clusters. Furthermore, the most populated cluster of the trajectory of 5-HT_{2A} simulated as a monomer preferentially recognizes antagonist structures. This can be certainly related to the fact that the monomeric 5-HT_{2A} is modeled on the basis of the resting state of the human β2-adrenergic receptor. Conversely, the most populated clusters of 5-HT_{2A} extracted from the heterodimeric simulation preferentially ranks 5-HT_{2A} agonist, and it is the structure that best recognize the HCs **(Figure 7B)**. These data must clearly be taken with caution and not overemphasized due to the short time of the MD simulation, nevertheless, a clear effect of the dimerization interface is appreciable. From one side, the presence of the heterodimeric interface induces a change in the binding pocket of 5-HT_{2A} switching the preference to 5-HT_{2A} agonists. From the other side, it seems that the homodimeric interface transmits anisotropic changes, with the two

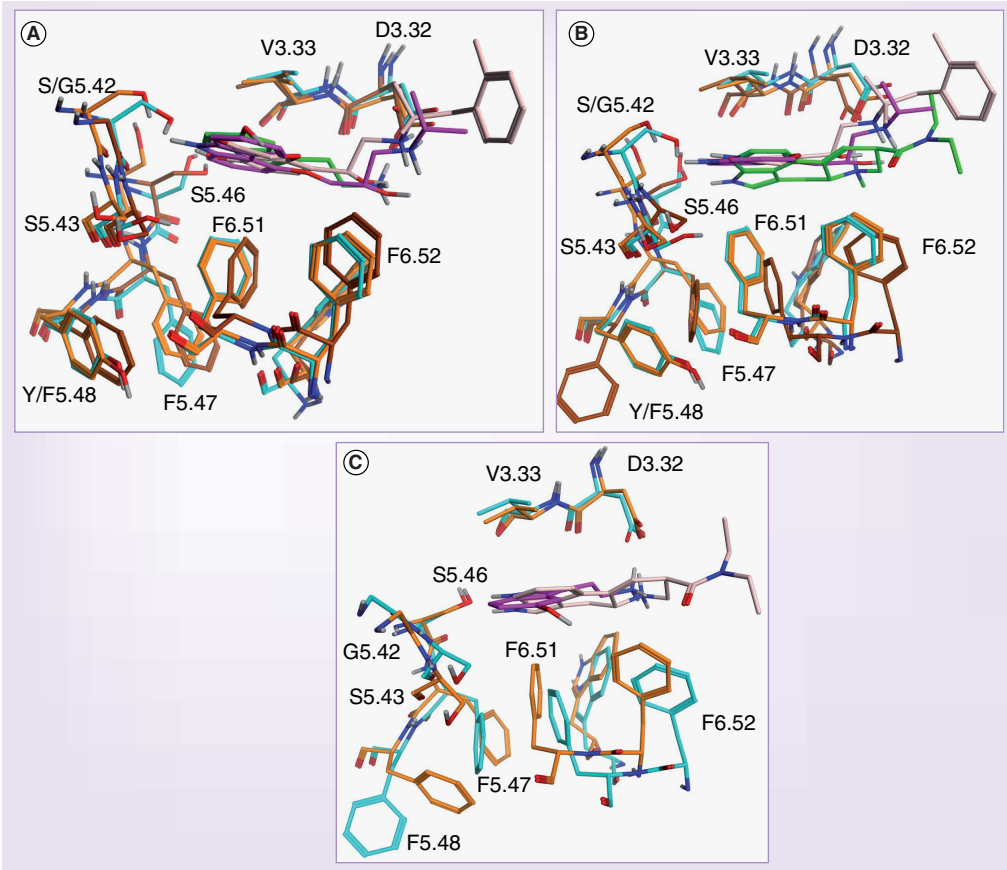

Figure 5. Results of the induced-fit docking of selected 5-HT$_{2A}$ ligands on different conformational states of the complex. (A) Comparison of the docking pose of serotonine in the representative structure of the first cluster with the x-ray crystal structures 2RH1 (carazolol/ β2-adrenergic receptor) and 3P0G (BI-167107/ β2-adrenergic receptor). The residues of 2RH1 are colored in orange, the residues of the 3P0G in cyan and the residue of the 5-HT$_{2A}$ receptor in brown. The carbazolol is highlighted in purple, the BI-167107 in pink and the serotonin in green. **(B)** Comparison of the docking pose of LSD in the representative structure of the most populated cluster with the x-ray crystal structures 2RH1 (carazolol/β2-adrenergic receptor) and 3P0G (BI-167107/ β2-adrenergic receptor). Residues and ligands are colored as described above. **(C)** Comparison of the docking poses for serotonin (purple) and LSD (pink) and the shape of the binding pocket of the representative structure of the first cluster (orange) and the representative structure of the most populated cluster (cyan), respectively.

protomers (ProA and ProB) behaving in a very different manner.

Conclusion

A growing body of experimental evidence indicates that GPCR aggregation, also among unrelated members of different subfamilies, is a relevant phenomenon for the physiological activity of these proteins [1–5,11–13]. In this work, we used MD simulations and docking studies to investigate the behavior of two GPCR complexes, namely the heterodimeric mGluR2–5-HT$_{2A}$ complex and the homodimeric 5-HT$_{2A}$–5-HT$_{2A}$ complex. Thus, the obtained results were compared also with those obtained by simulating the monomeric form of the 5-HT$_{2A}$ receptor. The aim of this work was to set up an experimental methodology for investigating the role of the dimerization interface in the topology of the binding pocket of 5-HT$_{2A}$. From MD simulations studies we were able to extract a set of receptor conformations by using cluster analysis. The shape of the binding pocket is tightly linked to the presence and to the type of a dimerization interface is clear from this study. In particular, the interface seems to significantly impact the flexibility of the CWxP microdomain-associated region on TM6, which is in turn responsible for shaping up a hydrophobic pocket conserved among members of class A GPCRs [47,48]. Our data suggest that this hydrophobic pocket is affected by the presence of the dimerization

interface and by the nature of the dimer partner. These changes in topology reflect a different ability of the heterodimer, homodimer, and monomer to rank a set of 5-HT_{2A} ligand docking studies. In particular, heterodimerization seems to allosterically induce a modification in the binding pocket of 5-HT_{2A}, which promote binding of 5-HT agonist and its ability to recognize HCs improves along the simulation, while homodimerization anisotropically affects the two identical 5-HT_{2A} protomers constituting the dimer. While this work was under review, new x-ray crystal structures of the turkey β1 and human β2-adrenergic receptors were disclosed [42–44], showing that an agonist produces at least three main effects: conformational changes of Ser5.43 and S5.46; conformational changes in TM5/TM6, and contraction of the binding pocket. Furthermore, the comparison of the new [42–45] and the previously published x-ray crystal structures of members the aminergic GPCRs subfamily shows that the binding pocket of agonists, antagonists, partial inverse agonists and inverse agonists is highly overlapped, with appreciable differences related to the interaction with the residues of Ser5.43 and S5.46. With our studies, we are able to detect conformational differences only at the Ser5.43 and S5.46 level, while the binding pocket of our structure increased in area and volume and we didn't see any conformational changes at TM5 level. This is likely due to the fact that the simulation time of our studies is too short to detect conformational changes at the helix level, and due to the fact that our simulations were carried out in the apo form of the receptor. Our studies clearly indicate that some flexible regions of the 5-HT_{2A} are affected by the presence of the dimerization interface and this impact the results of the docking studies.

Future perspective

As evidence on the role of hetero- or homodimerization in GPCR functioning increases, the need for computational procedures for simulating the effect of this process in ligand recognition will became more urgent. Long-scale MD simulations are likely to become a privileged tool to analyze the effect of the dimerization process, and the ability to extract information from these simulation will become central to the use of such approaches in an integrated drug-design effort in the GPCR field.

Supplementary data

Supplementary data accompany this paper and can be found at **www.future-science.com/doi/suppl/10.4155/FMC.11.27.**

Financial & competing interests disclosure

The authors have no relevant affiliations or financial involvement with any organization or entity with a financial interest in or financial conflict with the subject matter or materials discussed in the manuscript. This includes employment, consultancies, honoraria, stock ownership or

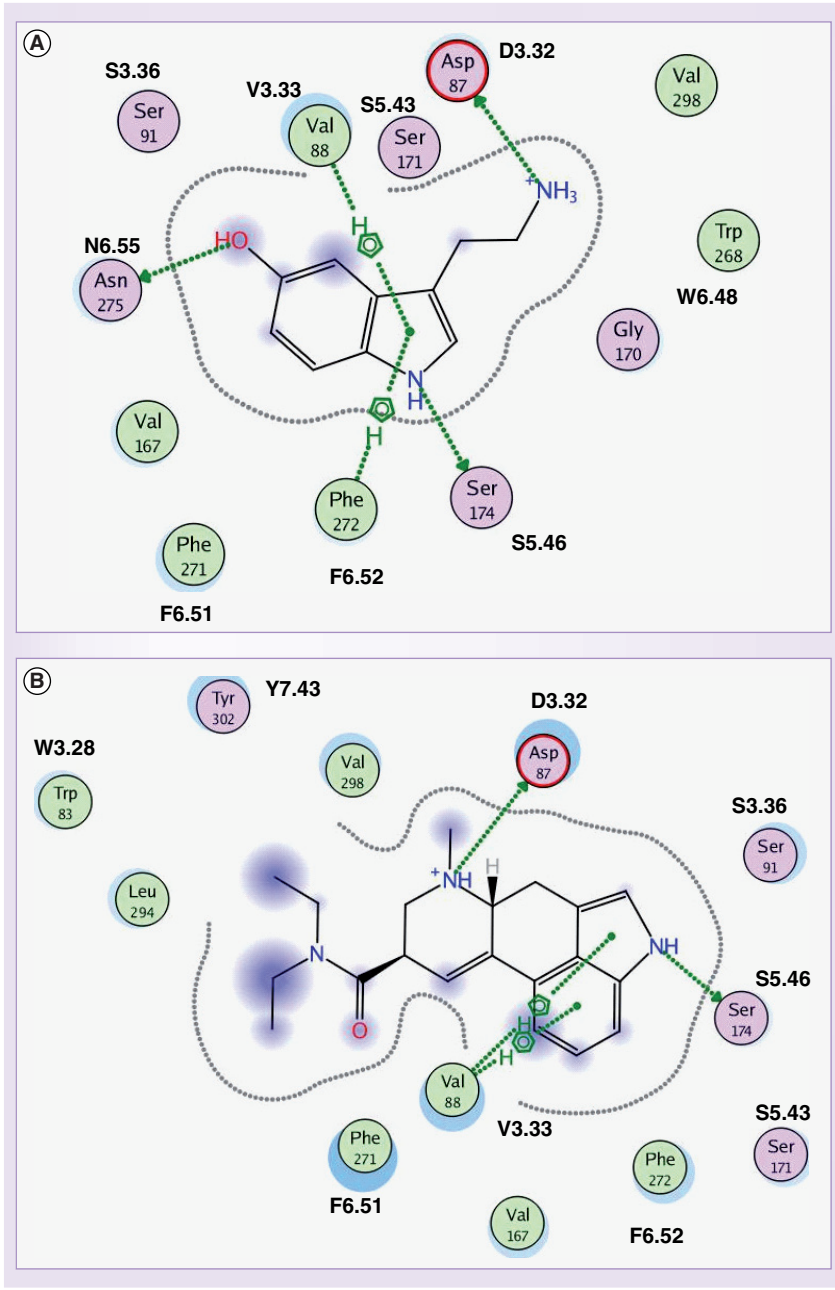

Figure 6. Map of the interaction between (A) serotonin and the 5-HT_{2A} receptor, and (B) LSD and the 5-HT_{2A} receptor.

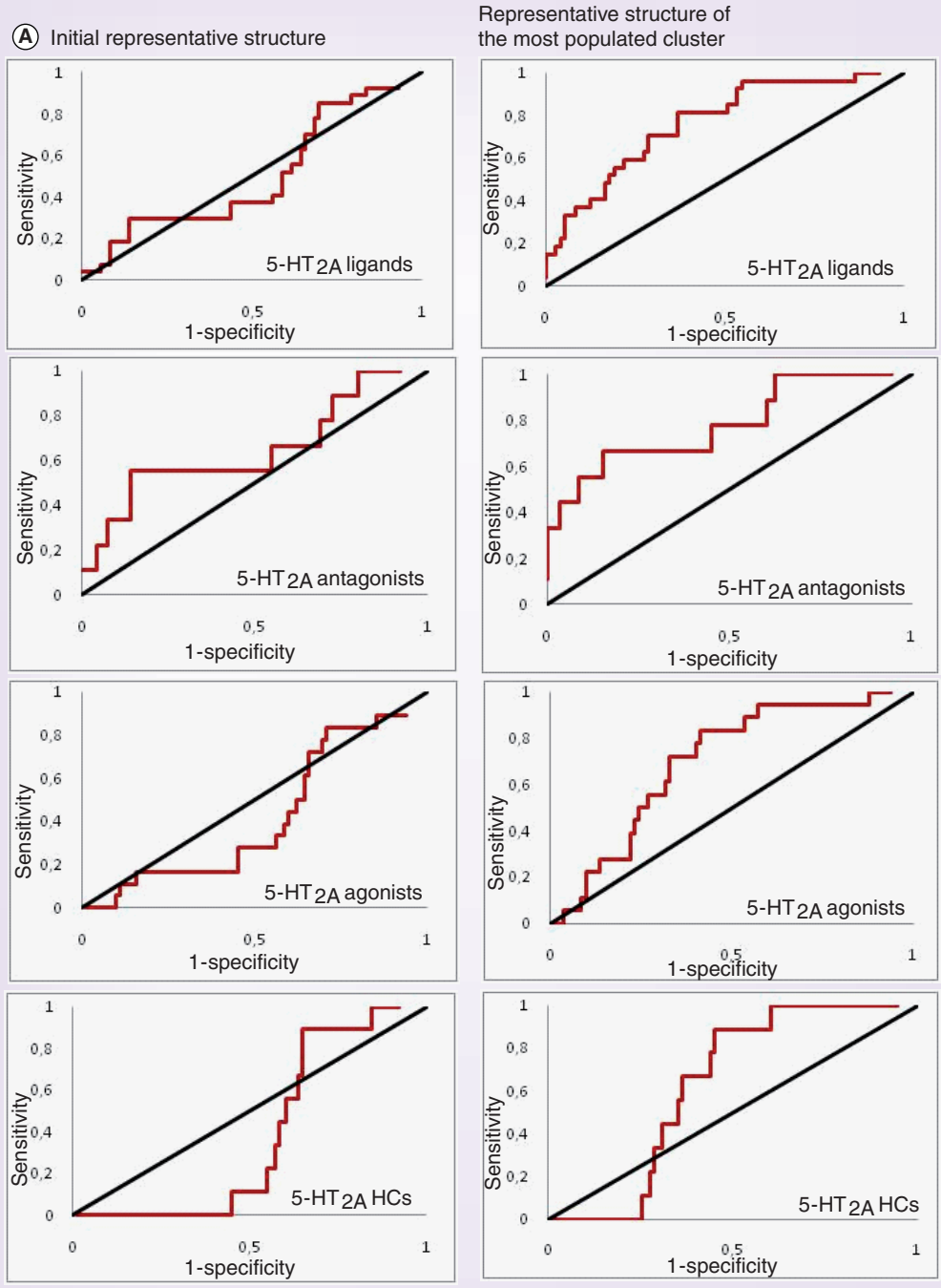

	Initial representative structure					Representative structure of the most populated cluster				
	AUC	EF 2%	EF 5%	EF 10%	EF 20%	AUC	EF 2%	EF 5%	EF 10%	EF 20%
5HT2A ligands	0.50	1.85	0.74	1.48	1.48	0.75	1.85	2.96	2.22	1.85
Antagonists	0.62	5.56	2.22	3.33	2.78	0.77	5.56	6.67	4.44	2.78
5HT2A agonists	0.43	0.00	0.00	0.56	0.83	0.68	0.00	1.11	1.11	1.39
5HT2AHCs	0.33	0.00	0.00	0.00	0.00	0.61	0.00	0.00	0.00	0,00

Figure 7. (A) Receiver operating characteristic curves and their statistical parameters for the monomeric form of the 5-HT$_{2A}$.

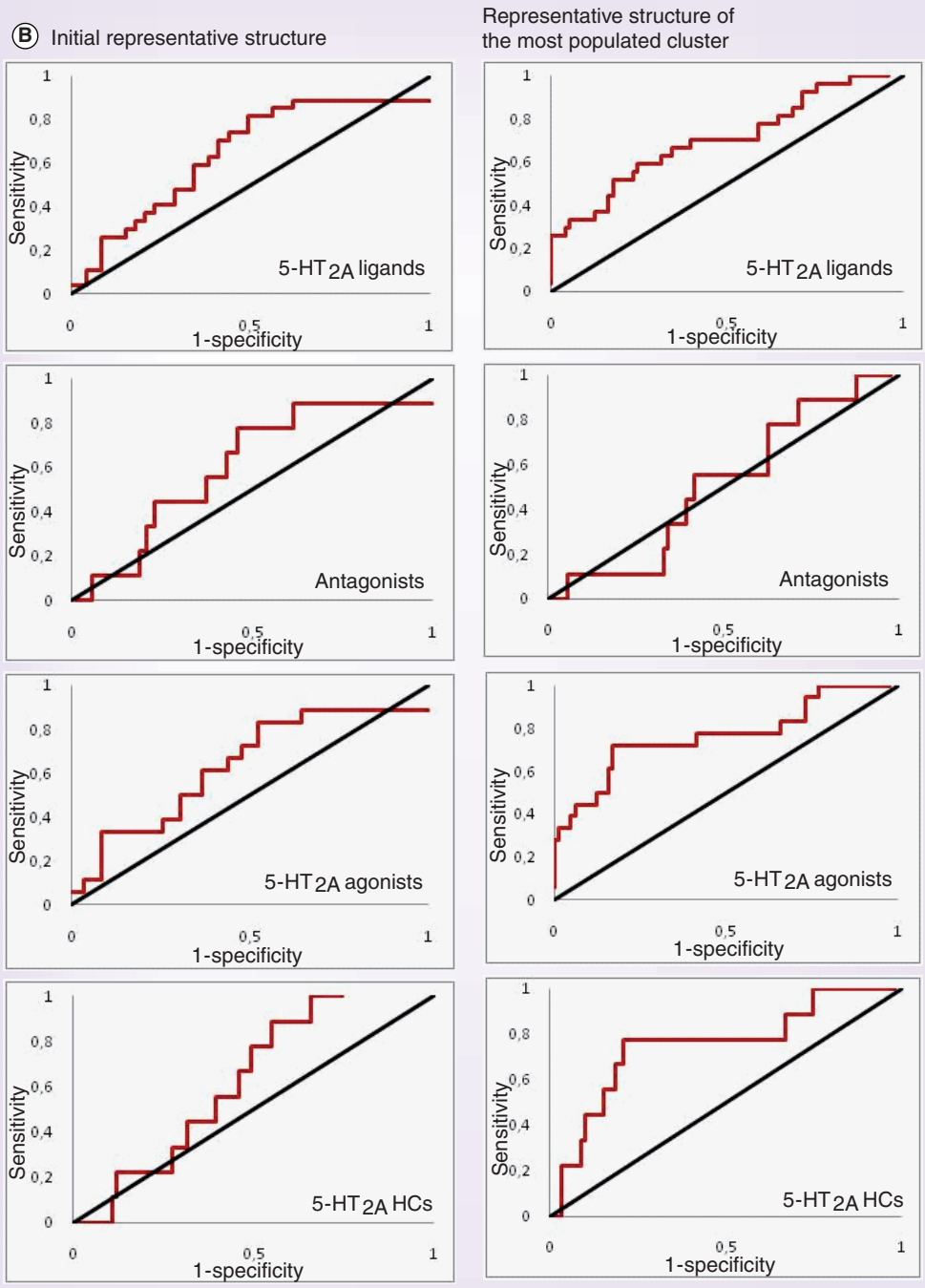

	Initial representative structure					Representative structure of the most populated cluster				
	AUC	EF 2%	EF 5%	EF 10%	EF 20%	AUC	EF 2%	EF 5%	EF 10%	EF 20%
5HT2A ligands	0.64	1.85	1.48	1.48	1.48	0.70	3.70	3.70	2.59	1.85
Antagonists	0.59	0.00	0.00	1.11	1.11	0.50	0.00	0.00	1.11	0.56
5HT2A agonists	0.63	2.78	2.22	1.67	1.67	0.76	5.56	5.56	3.33	2.50
5HT2AHCs	0.51	0.00	0.00	0.00	1.11	0.75	0.00	4.44	2.22	2.78

Figure 7 cont. (B) Receiver operating characteristiccurves and their statistical parameters for the heterodimeric form of the 5-HT$_{2A}$.

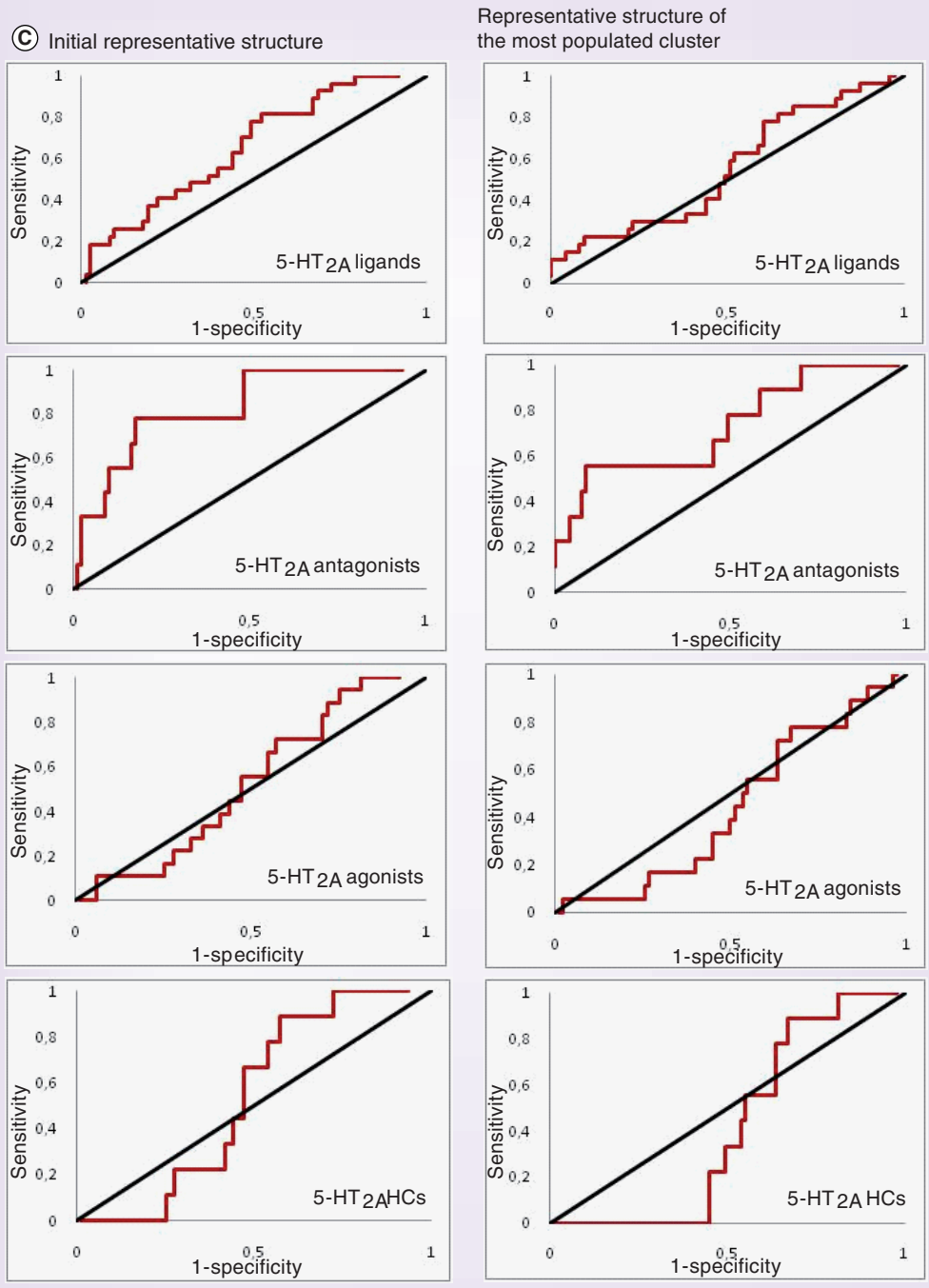

	Initial representative structure					Representative structure of the most populated cluster				
	AUC	EF 2%	EF 5%	EF 10%	EF 20%	AUC	EF 2%	EF 5%	EF 10%	EF 20%
5HT2A ligands	0.58	1.85	2.22	1.85	1.30	0.54	3.70	2.22	1.48	1.11
Antagonists	0.71	5.56	6.67	3.33	2.78	0.72	11.11	4.44	3.33	2.78
5HT2A agonists	0.52	0.00	0.00	1.11	0.56	0.43	0.00	1.11	0.56	0.28
5HT2AHCs	0.51	0.00	0.00	0.00	0.00	0.40	0.00	0.00	0.00	0.00

Figure 7 cont. (C) Receiver operating characteristic curves and their statistical parameters for the protomerA.

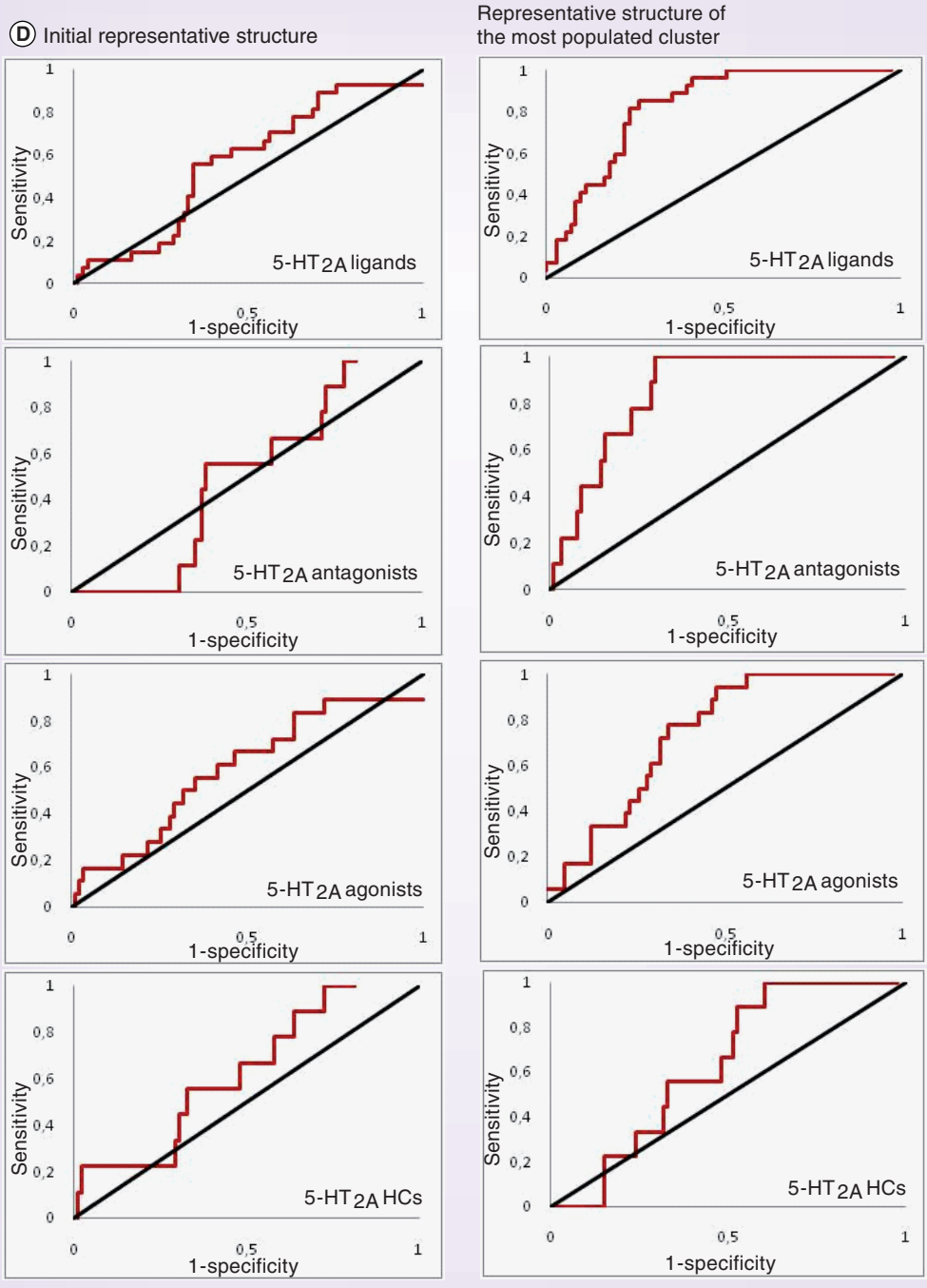

	Initial representative structure					Representative structure of the most populated cluster				
	AUC	EF 2%	EF 5%	EF 10%	EF 20%	AUC	EF 2%	EF 5%	EF 10%	EF 20%
5HT2A ligands	0.48	1.852	1.481	1.111	0.741	0.80	3.70	2.22	2.22	2.22
Antagonists	0.52	0.000	0.000	0.000	0.000	0.80	5.56	4.44	3.33	3.33
5HT2A agonists	0.57	2.778	2.222	1.667	1.111	0.70	2.78	1.11	1.67	1.67
5HT2AHCs	0.54	5.556	4.444	2.222	1.111	0.62	0.00	0.00	0.00	1.11

Figure 7 cont. (D) Receiver operating characteristic curves and their statistical parameters.

Executive summary

- Operational models of the mGluR2–5-HT_{2A} and 5-HT_{2A}-5-HT_{2A} dimeric complexes were constructed and simulated for 40-ns molecular dynamics.
- The dimer complexes constructed around a TM4–TM5 interface arrangement are stable under our simulation conditions.
- Molecular dynamics simulations and cluster analysis revealed asymmetric behavior of the protomers constituting the dimeric complexes.
- The dimerization interface clearly affects the topology of the binding pocket of 5-HT_{2A}.
- We identified microdomains on the 5-HT_{2A} structure responsible for the plasticity and flexibility of the receptor. These microdomains represent relevant structures for ligand recognition and the behavior of these microdomains is strongly affected by the nature of the dimerization interface.
- Docking studies and receiver operating characteristic curve analysis indicate that different conformational states of the receptor complexes are able to select individual subsets of 5-HT_{2A} ligands.
- This study describes a methodological procedure for incorporating the effect of receptor dimerization into drug-design efforts.

options, expert testimony, grants or patents received or pending, or royalties.

No writing assistance was utilized in the production of this manuscript.

Bibliography

Papers of special note have been highlighted as:
- ▪ of interest
- ▪▪ of considerable interest

1 Milligan G. The role of dimerisation in the cellular trafficking of G-protein-coupled receptors. *Curr. Opin. Pharmacol.* 10(1), 23–29 (2010).

▪ **Key review on the role of dimerisation in the G-protein coupled receptors (GPCRs) field.**

2 Albizu L, Cottet M, Kralikova M *et al.* Time-resolved FRET between GPCR ligands reveals oligomeric in native tissues. *Nat. Chem. Biol.* 6(8), 587–594 (2010).

▪▪ **Provides a key experimental evidence on the GPCRs dimerization in native tissues.**

3 Prezeau L, Rives ML, Comps-Agrar L, Maurel D, Kniazeff J, Pin JP. Functional crosstalk between GPCRs: with or without oligomerization. *Curr. Opin. Pharmacol.* 10(1), 6–13 (2010).

4 Wu B, Chien EY, Mol CD *et al.* Structures of the CXCR4 chemokine GPCR with small-molecule and cyclic peptide antagonists. *Science* 330(6007), 1066–1071 (2010).

▪ **Reports the crystal structures of trimeric GPCRs.**

5 Simpson LM, Taddese B, Wall ID, Reynolds CA. Bioinformatics and molecular modelling approaches to GPCR aligomerization. *Curr. Opin. Pharmacol.* 10(1), 30–37 (2010).

6 Smith NJ, Milligan G. Allostery at G protein-coupled receptor homo- and heteromers: uncharted pharmacological landscapes. *Pharmacol. Rev.* 62(4), 701–725 (2010).

7 Gonzàlez-Maeso J, Yuen T, Ebersole B *et al.* Transcriptome fingerprints distinguish hallucinogenic and nonhallucinogenic 5-hydroxytriptamine 2A receptor agonist effects in mouse somatosensory cortex. *J. Neurosci.* 23(26), 8836–8843 (2003).

8 Parrish JC, Braden MR, Gundy E, Nichols DE. Differential phospholipase C activation by phenylalkylamine serotonin 5-HT_{2A} receptor agonists. *J. Neurochem.* 95(6), 1575–1584 (2005).

9 Gonzàlez-Maeso J, Weisstaub NV, Zhou M *et al.* Hallucinogenes recruit specific cortical 5-HT_{2A} receptor-mediated signaling pathways to affect behavior. *Neuron.* 53(3), 439–452 (2007).

▪▪ **Differential effects of hallucinogens and nonhallucinogens on 5-HT_{2A} receptors.**

10 González-Maeso J, Sealfon SC. Agonist-trafficking and hallucinogens. *Curr. Med. Chem.* 16(8), 1017–1027 (2009).

11 Gonzalez-Maeso J, Ang RL, Yuen T *et al.* Identification of a serotonin/glutamate receptor complex implicated in psychosis. *Nature.* 452(7183), 93–97 (2008).

▪▪ **Evidence for heterodimeric form of 5-HT_{2A}.**

12 Gonzalez-Maeso J, Sealfon SC. Psychedelics and schizophrenia. *Trends Neurosci.* 32(4), 225–232 (2009).

13 Brea J, Castro M, Giraldo J *et al.* Evidence for distinct antagonist-revealed functional states of 5-hydroxytryptamine(2A) receptor homodimers. *Mol. Pharmacol.* 75(6), 1380–1391 (2009).

▪▪ **Evidence for a homodimeric form of 5-HT_{2A}.**

14 Rovira X, Vivó M, Serra J, Roche D, Strange PG, Giraldo J. Modelling the interdependence between the stoichiometry of receptor oligomerization and ligand binding for a coexisting dimer/tetramer receptor system. *Br. J. Pharmacol.* 156(1), 28–35 (2009).

15 McRobb FM, Capuano B, Crosby IT *et al.* Homology Modeling and docking evaluation of aminergic G protein-coupled receptors. *J. Chem. Inf. Model.* 50(4), 626–637 (2010).

16 Selent J, Lopez L, Sanz F, Pastor M. Multi-receptor binding profile of clozapine and olonzapine: a structural study based on the new beta2 adrenergic receptor template. *ChemMedChem* 3(8), 1194–1198 (2008).

17 Bruno A, Guadix AE, Costantino G. Molecular dynamics simulation of the heterodimeric mGluR2/5-HT_{2A} complex. An atomistic resolution study of a potential new target in psychiatric conditions. *J. Chem. Inf. Model.* 49(6), 1602–1616 (2009).

18 Humphrey W, Dalke A, Schulten K. VMD: visual molecular dynamics. *J. Mol. Graph.* 14(1), 33–38 (1996).

19 Shao J, Tanner SW, Thompson N, Cheatham TE III. Clustering molecular dynamics trajectories: 1. Characterizing the performance of different clustering algorithms. *J. Chem. Theory Comput.* 3(6), 2312–2334 (2007).

20 Vaidehi N. Dynamics and flexibility of G-protein-coupled receptor conformations and their relevance to drug design. *Drug Discov. Today* 15(21–22), 951–957 (2010).

21 Amaro R, Baron R, McCammon JA. An improved relaxed complex scheme for receptor flexibility in computer-aided drug design. *J. Comput. Aided Mol. Des.* 22(9), 693–705 (2008).

22 Mobarec JC, Filizola M. Advanced in the development and application of computational methodologies for structural modeling of G-protein coupled receptors. *Expert Opin. Drug Discov.* 3(3), 343–355 (2008).

23 Totrov M, Abagyan R. Flexible ligand docking to multiple receptor conformations: a practical alternative. *Curr. Opin. Struct. Biol.* 18(2), 178–184 (2008).

24 Kao HT, Adham N, Olsen MA, Weinshank RL, Branchek TA, Hartig PR. Site-directed mutagenesis of a single residue changes the binding properties of the serotonin 5-HT_2 receptor from a human to a rat pharmacology. *FEBS Lett.* 307(3),

324–328 (1992).

25 Roth BL, Shoham M, Choudhary MS, Khan N. Identification of conserved residues essential for agonist binding and second messenger production at 5-hydroxytriptamine2A receptors. *Mol. Pharmacol.* 52(2), 259–266 (1997).

26 Roth BL, Willins DL, Kristiansen K, Kroeze WK. 5-hydroxytryptamine2-family receptors (5-hydroxytryptamine2A, 5-hydroxytryptamine2B, 5-hydroxytryptamine2C): where structure meets function. *Pharmacol. Ther.* 79(3), 231–257 (1998).

27 Shapiro DA, Kristiansen K, Kroeze WK, Roth BL. Differential modes of agonist binding to 5-hydroxytryptamine(2A) serotonin receptors revealed by mutation and molecular modeling of conserved residues in transmembrane region 5. *Mol. Pharmacol.* 58(5), 877–886 (2000).

28 Kristiansen K, Kroeze WK, Willins DL *et al.* A highly conserved aspartic acid (Asp-155) anchors the terminal amine moiety of tryptamines and is involved in membrane targeting of the 5-HT(2A) serotonin receptor but does not participate in activation via a "salt-bridge disruption" mechanism. *J. Pharmacol. Exp. Ther.* 293(3), 735–746 (2000).

29 Ebersole BJ, Visiers I, Weinstein H, Sealfon SC. Molecular basis of partial agonism: orientation of indoleamine ligands in the binding pocket of the human serotonin 5-HT_{2A} receptor determines relative efficacy. *Mol. Pharmacol.* 63(1), 36–43 (2003).

30 Braden MR, Nichols DE. Assessment of the roles of serines 5.43(239) and 5.46(242) for binding and potency of agonist ligands at the human serotonin 5-HT_{2A} receptor. *Mol. Pharmacol.* 72(5), 1200–1209 (2007).

31 Blaazer AR, Smid P, Kruse CG. Structure–activity relationship of phenylalkylamines as agonist ligand for 5-HT_{2A} receptors. *ChemMedChem.* 3(9), 1299–1309 (2008).

32 Ballestreros JA, Weinstein H. Integrated methods for the construction of three-dimensional models and computational probing of structure–function relations in G protein coupled receptors. *Methods Neurosci.* 25, 366–428 (1995).

33 Okuno Y, Tamon A, Yabuuchi H *et al.* GLIDA: GPCR-ligand database for chemical genomics drug discovery – database and tools update. *Nucleic Acids Res.* 36(Suppl. 1) D907–D912 (2008).

34 Rabin RA, Regina M, Doat M, Winter JC. 5-HT_{2A} receptor-stimulated phosphoinositide hydrolysis in the stimulus effects of hallucinogens. *Pharmacol. Biochem. Behav.* 72(1–2), 29–37 (2002).

35 Newman-Tancredi A, Cussac D, Quentric Y *et al.* Differential actions of antiparkinson agents at multiple classes of monoaminergic receptor. III. Agonist and antagonist properties at serotonin, 5-HT1 and 5-HT_2, receptor subtypes. *J. Pharmacol. Exp. Ther.* 303(2), 815–822 (2002).

36 Nelson DL, Lucaites VL, Wainscott DB, Glennon RA. Comparisons of hallucinogenic phenylisopropylamine binding affinities at cloned human 5-HT_{2A}, 5-HT_{2B} and 5-HT_{2C} receptors. *Naunyn Schmiedebergs Arch. Pharmacol.* 359(1), 1–6 (1999).

37 Knight AR, Misra A, Quirk K *et al.* Pharmacological characterisation of the agonist radioligand binding site of 5-HT_{2A}, 5-HT_{2B} and 5-HT_{2C} receptors. *Naunyn Schmiedebergs Arch. Pharmacol.* 370(2), 114–123 (2004).

38 Seeman P, Kapur S. Atypical antipsychotics. Mechanism of action. *Br. J. Psychiatry.* 180, 465–466 (2002).

39 Cussac D, Boutet-Robinet E, Ailhaud MC *et al.* Agonist-directed trafficking of signalling at serotonin 5-HT_{2A}, 5-HT_{2B} and 5-HT_{2C}-VSV receptors mediated Gq/11 activation and calcium mobilisation in CHO cells. *Eur. J. Pharmacol.* 594(1–3), 32–38 (2008).

40 Richelson E, Souder T. Binding of antipsychotic drugs to human brain receptors – focus on newer generation compounds. *Life Sci.* 68(1), 29–39 (2000).

41 Friesner RA, Banks JL, Murphy RB *et al.* Glide: a new approach for rapid, accurate docking and scoring. 1. Method and assessment of docking accuracy. *J. Med. Chem.* 47(7), 1739–1749 (2004).

42 Rasmussen SGF, Choi H-J, Fung JJ *et al.* Structure of a nanobody-stabilized active state of the β2-adrenoceptor. *Nature* 469(7329), 175–180 (2011).

▪▪ **Describes the GPCR active state complexed with an agonist and camelid antibody fragment with Gα-like behavior.**

43 Rosembaum DM, Zhang C, Lyons JA *et al.* Structure and function of an irreversible agonist- β_2-adrenoceptor complex. *Nature* 469(7329), 236–240 (2011).

▪▪ **Describes the GPCR active state covalently linked to an agonist.**

44 Warne T, Moukhametzianov R, Baker JC *et al.* The structural basis for agonist and partial agonist action on a β_1-adrenergic receptor. *Nature* 469(7329), 241–244 (2011).

45 Chien EY, Liu W, Zhao Q *et al.* Structure of the human dopamine D_3 receptor in complex with a D_2/D_3 selective antagonist. *Science* 330(6007), 1091–1095 (2010).

46 Sonego P, Kocsor A, Pongor S. ROC analysis: applications to the classification of biological sequences and 3D structures. *Brief. Bioinformatics* 9(3), 198–209 (2008).

47 Reggio PH. Computational methods in drug design: modeling G protein-coupled receptor monomers, dimers, and oligomers. *AAPS J.* 8(2), E322–336 (2006).

48 Lagerstrom MC, Schioth HB. Structural diversity of G protein-coupled receptors and significance for drug discovery. *Nat. Rev. Drug Discov.* 7(4), 339–357 (2008).

■ Websites

101 University of Utah Cheatham laboratory. Software links. http://www.chpc.utah.edu/~cheatham/software.html

102 GLIDA: GPCR-Ligand Database. http://pharminfo.pharm.kyoto-u.ac.jp/services/glida/

103 Schrodinger. www.schrodinger.com

104 IUPHAR database. www.iuphar-db.org/DATABASE/ReceptorFamiliesForward?type=GPCR

105 Computer atlas of surface topography of proteins. http://sts-fw.bioengr.uic.edu/castp/calculation.php